Langmuir **2003,** *19,* 2763−2767

Micro- and Macro-Tribological Study on a Self-Assembled Dual-Layer Film

Sili Ren,[†,‡] Shengrong Yang,[*,†] and Yapu Zhao[‡]

State Key Laboratory of Solid Lubrication, Lanzhou Institute of Chemical Physics, Chinese Academy of Sciences, Lanzhou 730000, China and State Key Laboratory of Nonlinear Mechanics, Institute of Mechanics, Chinese Academy of Sciences, Beijing 100080, China

Received October 7, 2002. In Final Form: December 12, 2002

A novel self-assembled dual-layer film as a potential excellent lubricant for micromachines was successfully prepared on single-crystal silicon substrate by chemical adsorption of stearic acid (STA) molecules on self-assembled monolayer of 3-aminopropyltriethoxysilane (APS) with terminal amino group. The structure and morphology of the film were characterized by means of contact-angle measurement, ellipsometric thickness measurement, Fourier transformation infrared spectrometric analysis, and atomic force microscopic analysis. The micro- and macro-tribological properties of the dual-layer film were investigated as well. As the results, the dual-layer STA−APS film was hydrophobic with the contact angle for water to be about 98° and the overall thickness about 2.2 nm. Atomic force microscopic images showed that the APS surface was characterized by defects such as small grains and holes; it became relatively smooth and homogeneous after the self-assembly of the STA film. The STA−APS film possessed good adhesive resistance and could greatly reduce the micro- and macrofriction force. Moreover, it registered better load-carrying capacity and antiwear ability than the self-assembled monolayer of octadecyltrichlorosilane (OTS) in sliding against the ceramic counterface. Thus, the dual-layer self-assembled film might find promising application in the lubrication of micro-electromechanical systems (MEMS).

1. Introduction

The fast developing micro-electromechanical systems are known for their superior performance and low unit cost.[1,2] However, the large surface-area-to-volume ratios raise serious adhesive and frictional problems for their operations.[3] Owing to the microsize of the MEMS components, conventional lubricants are no longer the most desirable ones. Since silicon, polysilicon, silicon carbide, and other ceramic materials are the main materials to build these systems,[2] SAMs derived from alkylsilanes have been the emphasis in the studies of resolving the tribological problems of MEMS.[4−13]

Srinivasan and co-workers[12] investigated the stiction of SAMs derived from the precursor molecules of octadecyltrichlorosilane (OTS) and (1H, 1H, 2H, 2H)-perfluorodecyltrichlorosilane (FDTS) which were used as boundary lubricants in polycrystalline silicon microstructures. They found that the release-related stiction associated with water capillary forces was eliminated because of the hydrophobicity of these SAMs, and the in-use stiction was also greatly reduced. Adhesive experiments demonstrated that the SAM of OTS reduced adhesion by more than 3-fold over the conventional process and the fluorinated SAMs further reduced it by 4 times. Tsukruk and co-workers investigated the nanotribological properties of the SAMs of hexadecyltrichlorosilane by means of friction force microscopy (FFM) and found that the monolayer greatly reduced the friction coefficient and no signs of wear were observed.[11] They accordingly suggested that the alkylsilane monolayers were very robust and stable and displayed only elastic deformation under high shear forces, which was also reported elsewhere.[10,14] Such a supposition, however, was disputed by other observations. For example, Patton et al.[13] found that the OTS monolayer could be easily worn although it could broaden the motor's operating envelope to a long range of humidity. Cha and Kim investigated the macroscopic tribological properties of OTS monolayer using a pin-on-disk test rig and found that the monolayer as a lubricant functioned well for loads below 100 mN but was liable to wear for loads above 100 mN (100 mN corresponds to 0.6 Gpa for nominal contact pressures).[5] Similar results were also reported elsewhere.[15,16]

To further improve the tribological behavior of the SAMs of alkylsilanes and to acquire insights into their potential in resolving the tribological problems of MEMS, we prepared a self-assembled dual-layer film by making use of the chemical adsorption of the stearic acid molecules onto the SAMs of 3-aminopropyltriethoxysilane(APS) on single-crystal silicon surface. The tribological behavior of the resulting dual-layer film was comparatively investigated using the OTS monolayer as a reference. The dual-

* Corresponding author. E-mail: sryang@licp.ac.cn.
† Lanzhou Institute of Chemical Physics.
‡ Institute of Mechanics.

(1) Wen, S.-Z. *Nanotribology*; Qinghua University: Beijing, 1990; pp 1−4 (in Chinese).
(2) Spearing, S. M. *Acta Mater.* **2000,** *48,* 179.
(3) Rymuza, Z. *Microsystem Technologies* **1999,** *5,* 173.
(4) Maboudian, R.; Ashurst, W. R.; Carraro, C. *Sens. Actuators* **2000,** *82,* 219.
(5) Cha, K. H.; Kim, D. E. *Wear* **2001,** *251,* 1169.
(6) Gauthier, S.; Aimé, J. P.; Bouhacina, T.; Attias, A. J.; Desbat, B. *Langmuir* **1996,** *12,* 5126.
(7) Clear, S. C.; Nealey, P. F. *Langmuir* **2001,** *17,* 720.
(8) Carpick, R. W.; Salmeron, M. *Chem. Rev.* **1997,** *97,* 1163.
(9) Bhushan, B.; Kulkarni, A. V.; Koinkar, V. N.; Boehm, M.; Odoni, L.; Martelet, C.; Belin, M. *Langmuir* **1995,** *11,* 3189.
(10) Bliznyuk, V. N.; Everson, M. P.; Tsukruk, V. V. *J. Tribology* **1998,** *120,* 489.
(11) Tsukruk, V. V.; Everson, M. P.; Lander, L. M.; Brittain, W. J. *Langmuir* **1996,** *12,* 3905.
(12) Srinivasan, U.; Houstonm, M. R.; Howe, R. T.; Maboudian, R. *J. Microelectromech. Syst.* **1998,** *7,* 252.
(13) Patton, S. T.; Cowan, W. D.; Eapen, K. C.; Zabinski, J. S. *Tribology Lett.* **2001,** *9,* 199.
(14) DePalma, V.; Tillman, N. *Langmuir* **1989,** *5,* 868.
(15) Rye, R. R.; Nelson, G. C.; Dugger, M. T. *Langmuir* **1997,** *13,* 2965.
(16) Ren, S.-L.; Yang, S.-R.; Zhao, Y.-P.; Zhou, J.-F.; Xu, T.; Liu, W.-M. *Tibology Lett.* **2002,** *13,* 233.

10.1021/la026662e CCC: $25.00
Published on Web 02/27/2003

layer film showed better friction-reducing and antiwear ability than the OTS monolayer and might find promising application in the lubrication of MEMS.

2. Experimental Section

Materials. Polished single-crystal silicon (111) wafers (obtained from GRINM Semiconductor Materials Co., Ltd., Beijing) with a surface roughness of about 0.4 nm after cleaning were used as the substrate. 3-aminopropyltriethoxysilane (APS; 99%) was obtained from ACROS (New Jersey, USA). Stearic acid (STA) and *N,N′*-dicyclohexylcarbodiimide (DCCD) (Sheshan Chemical, Shanghai, China) were of analytical purity and used after purification. The solvents *n*-hexane (purity >98%) and toluene (99.5%, anhydrous) were used as received.

Preparation of the Self-Assembled Films. Silicon wafers were cleaned and hydroxylated by immersing in a piranha solution (a mixture of 7:3 (V/V) 98%H_2SO_4 and 30%H_2O_2) at 90 °C for 30 min. The wafers were then fully rinsed with ultrapure water, placed into the APS solution of 5.0×10^{-3} M in a mixed solvent of acetone and ultrapure water (v/v = 5:1), and held there for 12 h. The target monolayer of APS was thus formed on the hydroxylated silicon surface. After rinsing with ultrapure water, the APS-coated silicon substrates were put into a dilute solution of STA and DCCD in *n*-hexane and kept for 24 h. DCCD which would not adsorb onto the coated Si surface was used here as a dehydrated reagent to accelerate the reaction between STA and APS. A monolayer of STA is presumably produced on the top of the APS film since the terminal amino groups in APS can react with the carboxyl groups in STA to form chemical bonds. The resulting dual-layer film samples were washed sequentially with *n*-hexane, acetone, and ultrapure water, to get rid of the physical adsorbed impurities.

Characterization of the Films. The static contact angles for ultrapure water on the films were measured with a Kyowa contact-angle meter. At least five replicate measurements were carried out for each specimen, and the measurement error was below 2°.

The thickness of the films was measured on a Gaertner L116-E ellipsometer, which was equipped with a He–Ne laser (632.8 nm) set at an incident angle of 70°. A real refractive index of 1.45 was assumed for all the films. Five replicate measurements were carried out for each specimen and the thickness was recorded to an accuracy of ±0.3 nm.

Fourier transformation infrared spectra were recorded on an IFS66V Fourier transformation infrared spectrometer. By using transmission mode, spectrum was collected for 500 scans at a resolution of 4 cm^{-1}. To eliminate or decrease the interfering of H_2O and CO_2, the sample chamber and optical chamber was vacuumed to 3 mbar. The freshly cleaned single-crystal silicon wafer was used as the reference.

A SPA400 (Seiko Instruments Inc.) atomic force microscope (AFM) was used to observe the film morphology, using "tapping scanning" mode.

The nanotribological behavior of the dual-layer film was characterized with an AFM/FFM controlled by RHK electronics (RHK Technology, Rochester Hills, MI), using the contact mode. Commercially available Si_3N_4 cantilevers/tips with a nominal force constant of 0.5 N/m and tip radius of less than 50 nm (Park Instruments, Sunnyvale, CA) were employed. To obtain the adhesive force between the AFM tip and the film surface, the force–distance curve was recorded and the pull off force reckoned as the adhesive force, which was given by

$$F = K_c \Delta Z_p$$

where K_c is the force constant of the cantilever and ΔZ_p is the vertical displacement of the piezotube, that is, the deflection of the cantilever.[17,18] In the inset of Figure 4, a typical force–distance curve was shown. The displacement of the retraction part from approach part because of the hysteresis of piezotube would be adjusted. All the friction and adhesion tests were conducted at room temperature of ~21 °C and a relative humidity of 65%.

(17) Xiao, X. D.; Qian, L. M. *Langmuir* **2000**, *16*, 8153.
(18) Tsukruk, V. V.; Bliznyuk, V. N. *Langmuir* **1998**, *14*, 446.

Table 1. Contact Angle and Thickness for the Silica Layer and the Modified Si Surfaces

surface	contact angle (°)	thickness (nm)
SiO_2/Si	~0	~2.0
APS	44.0	0.5
STA	98.0	1.7

The macro-tribological behavior of the dual-layer film was evaluated on a DF–PM unidirectional sliding tribometer. The details of the tribometer were availed elsewhere.[19] Briefly, the lower specimen slides at a speed of 90 mm/min for a distance of 7 mm, under selected normal load applied to the stationary ball by an arm attached to a dead weight; then, it stops at the end of each sliding pass and keeps off contact with the upper ball and returns to the original starting position, followed by the same repetitive procedures. The counterpart ball was made of Si_3N_4 (ϕ 4 mm) with rms roughness of about 8.6 nm. Prior to the test, the ceramic ball was cleaned with acetone-soaked cotton. Loads of 0.5, 1, and 2 N were selected and the corresponding initial Hertzian contact stresses were estimated to be about 0.7, 0.9, and 1.1 GPa, respectively. The friction coefficient and sliding cycles were recorded automatically. It was assumed that lubrication failure of the film occurred as the friction coefficient rose sharply to a higher and stable value similar to that of a cleaned silicon wafer against the same counterface (about 0.65). The number of sliding cycles at this point was recorded as the wear life of the film. All the tests were conducted at room temperature (25 °C) and a relative humidity of 45%.

The morphologies of the worn film surfaces were observed with a JSM-5600LV scanning electron microscope (SEM).

3. Results and Discussion

3.1 Structure and Morphology Characterization. Contact-angle measurement is effective to reflect the variation of solid-surface chemical composition. The contact angles for water on the hydroxylated silicon surface and the self-assembled films thereon are shown in Table 1. Naturally, the hydroxylated silicon surface and the APS monolayer thereon are hydrophilic, with the water-contact angles about 0° and 44.0°, respectively, which agree well with what have been reported.[20,21] Once the STA layer was chemically adsorbed onto the APS monolayer, the contact angle greatly increases to 98° and the resulting dual-film surface becomes hydrophobic. The results of ellipsometric thickness measurement are also listed in Table 1. After hydoxylating in the piranha solution at 90 °C for 30 min, a silica layer of about 2.0-nm thick is generated on the silicon wafer. The thickness for the single APS and STA layer is about 0.5 and 1.7 nm, respectively. The variation of the contact angles and the thickness indicates that STA molecules have successfully adsorbed onto the APS-coated silicon surface. The APS monolayer with terminal amino group are ready to react with the carboxylic acid in the presence of DCCD as a dehydrating agent, on the basis of the covalent amide bond between the STA and APS molecules. The reaction process is schematically shown in Figure 1. However, both the contact angle (98°) and the thickness (1.7 nm) measured for the STA layer in the present work are a little bit smaller than that for the STA SAMs on Al reported elsewhere.[22] This indicates that the derivatization of the APS might be incomplete and the STA molecules in the film might be packed in a contorted or slantwise state.

The transmission infrared spectrum of the STA–APS dual-layer film in the frequency range of 3000–2800 cm^{-1}

(19) Yu, L.-G.; Zhang, P.-Y.; Du, Z.-L. *Surf. Coat. Technol.* **2000**, *130*, 110.
(20) Chen, K.; Caldwell, B.; Mirkin, C. A. *J. Am. Chem. Soc.* **1993**, *115*, 1193.
(21) Caldwell, W. B.; Chen, K.; Mirkin, C. A.; Babinec, S. J. *Langmuir* **1993**, *9*, 1945.
(22) Tao, Y. T. *J. Am. Chem. Soc.* **1993**, *115*, 4350.

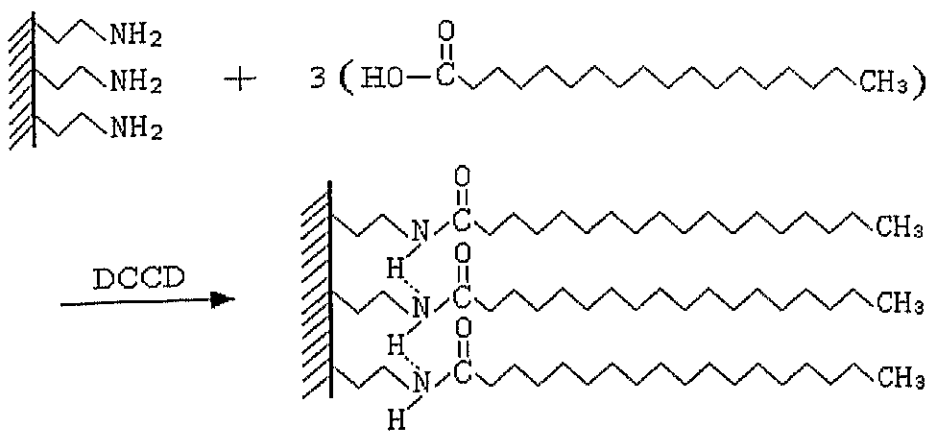

Figure 1. Schematic structure and forming process of STA molecules chemically adsorbing onto APS monolayer surface.

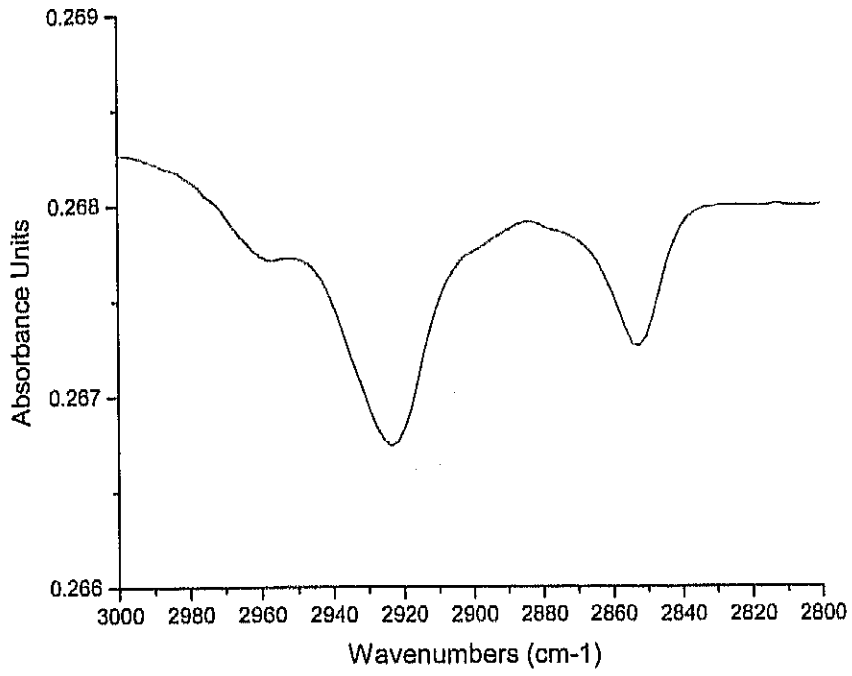

Figure 2. Transmission IR spectrum for STA–APS film on silicon wafer in the high-frequency region.

is shown in Figure 2. It can be seen that the peak frequencies for asymmetric and symmetric methylene vibrations, ν_{as} (CH_2) and ν_s (CH_2), appear at 2923 cm^{-1} and 2853 cm^{-1}, respectively. The amide I~III bands should appear in the frequency range of 1700–1200 cm^{-1} if the process shown in Figure 1 does occur. However, because of the weak signal, it is hard to distinguish them from the interfering peaks assigned to H_2O molecules and the silicon substrate.

Figure 3 shows the AFM morphological images of APS monolayer and STA–APS dual-layer films. Some holes and grains are seen on the APS surface (Figure 3a), which might come from the silicon wafers themselves or the polymerization of APS in solution and deposited onto the surface. After the generation of the STA layer, the film surface becomes relatively smooth and homogeneous (Figure 3b). The root-mean-square (rms) microroughness of the monolayer is estimated to be 0.34 nm over an area of 2 μm × 2 μm, which is a little bit lower than the 0.45 nm of the APS monlayer surface. These observations indicate that the adsorption of the STA molecules onto the APS surface helps to improve the surface quality.

3.2 Micro-Tribological Behavior Characterization. The adhesive forces between the AFM tip and the film surfaces are shown in Figure 4. Strong adhesion is observed on the hydroxylated silicon surface, on which the adhesive force is as high as about 72 nN. Once the APS monolayer and STA–APS dual-layer film are generated, the adhesive forces are greatly decreased to 24 nN and 5 nN, respectively. This indicates that the STA–APS dual-layer film has good adhesion-resistance. It is also observed that the adhesive forces are closely related to the contact angles shown in Table 1. In other words, the adhesive force greatly decreases with increasing hydrophobicity of the surface. Such phenomenon is well understood, since the adhesion dominated by the capillary

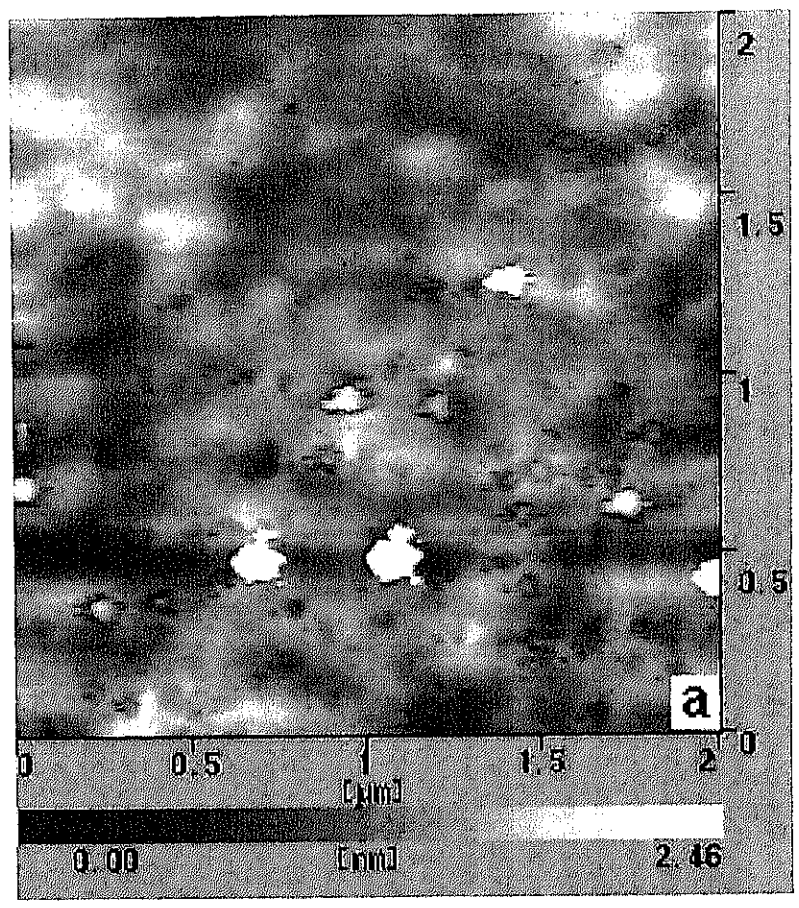

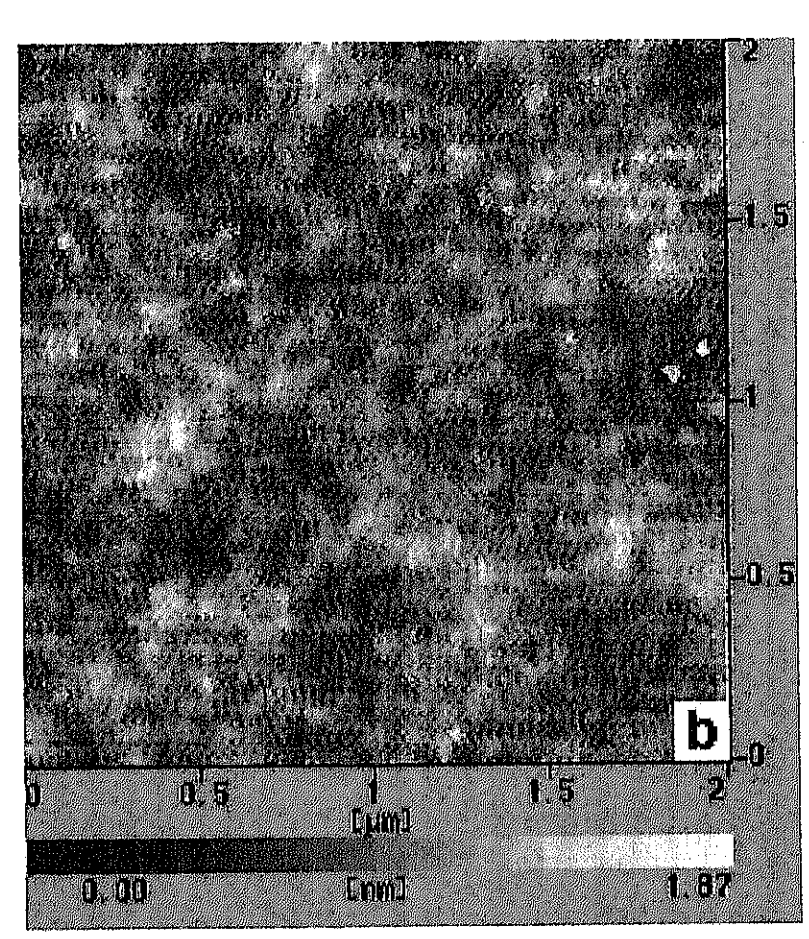

Figure 3. AFM topographic images of APS monolayer (a) and STA–APS dual-layer film (b) on silicon surface.

force between the tip and the surface is dramatically lowered or even eliminated when the surface becomes hydrophobic.

To obtain stable friction-versus-load curves especially on the silicon surface, a typical blunting process of a Si_3N_4 tip via friction scanning on mica was made in a similar manner as reported.[23] The friction-versus-load curves for the hydroxylated silicon surface, APS monolayer, and STA–APS dual-layer film measured using the blunt tip are shown in Figure 5. It is rational to observe that both the two films greatly reduce the friction force; especially, the STA–APS dual-layer film possesses much better lubricity. This is because the long chains of STA molecules with one end attached to the substrate surface have a significant freedom to swing and rearrange along the sliding direction under shear stress and therefore yield a smaller resistance. Besides, the low friction of the STA–APS dual-layer film could also be attributed to the lower surface energy. Moreover, large nonzero friction signal is

(23) Xiao, X. D.; Qian, L. M.; Wen, S. Z. *Langmuir* **2000**, *16*, 662.

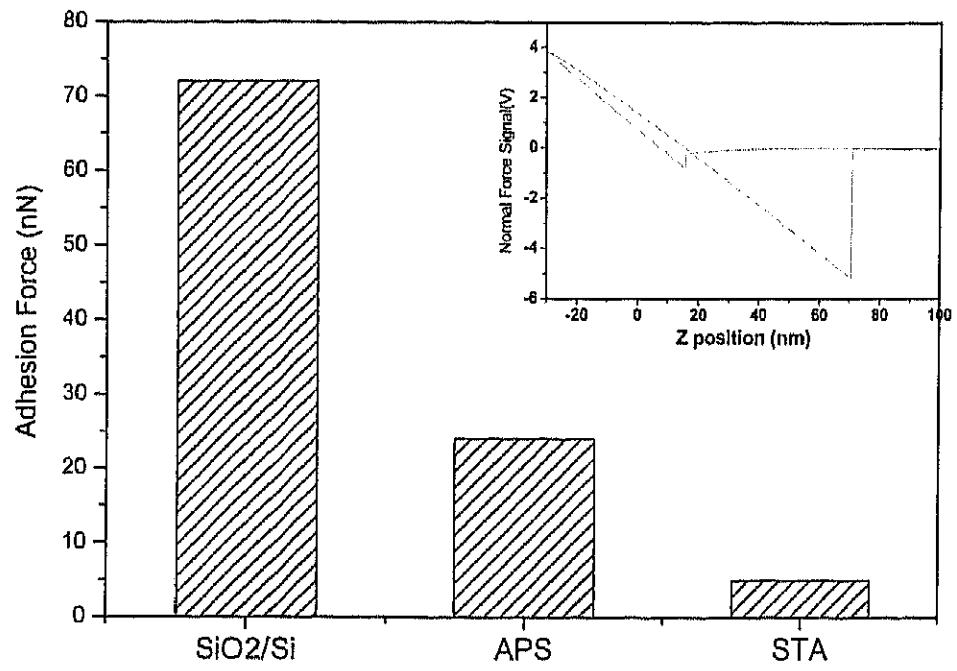

Figure 4. Adhesive forces between an AFM tip and the surfaces of the hydroxylated silicon (SiO_2/Si), APS monolayer, and STA–APS dual-layer film (RH = 65%). The inset shows a typical approach retract force–distance curve.

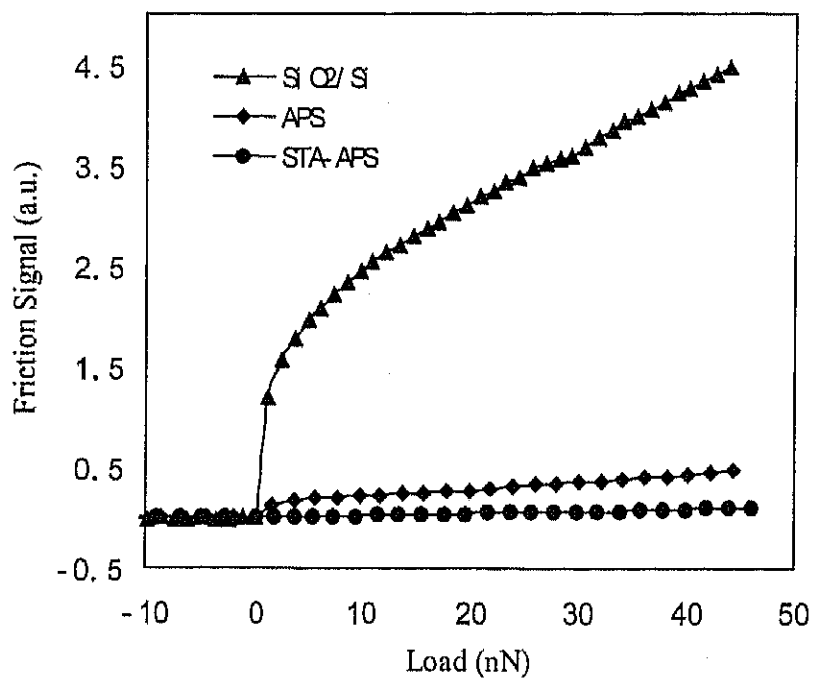

Figure 5. Friction-versus-load curves for surfaces of the hydroxylated silicon (SiO_2/Si), APS monolayer, and STA–APS film at a scanning velocity of 0.5 μm/s (RH = 65%).

observed at zero external load for the hydroxylated silicon surface, which is attributed to the jump-to-contact instability caused by attractive forces during the approach of the tip to the sample surface. This reflects that the silicon surface has large surface energy. The friction curve for the silicon surface is convex-shaped in the low-load region up to 15 nN, while above 15 nN the friction force increases linearly with increasing external load. The above observation could be explained by taking into account the adhesion between the tip and the surface. Considering the adhesion, $F_f(F_n)$ behavior can be described in a general form:[18]

$$F_f = C_1 F_n^{\,m} + C_2 F_n + C_3$$

where F_f and F_n are the friction force and external load, respectively. C_1, C_2, and C_3 are material-dependent constants, and the index m ($0 < m < 1$) depends on the asperity shape ($m = 2/3$ for sphere/plane contact). The first term in the equation is closely related to the adhesion of interacting surfaces. Then, it is well understood that the friction curve for the Si substrate is convex-shaped in the low-load region, considering the contribution of the strong adhesion on silicon surface as shown in Figure 4. With the normal loads increasing, the adhesion fraction of the friction force will relatively decrease as compared to the shear fraction determined by the normal load; thus,

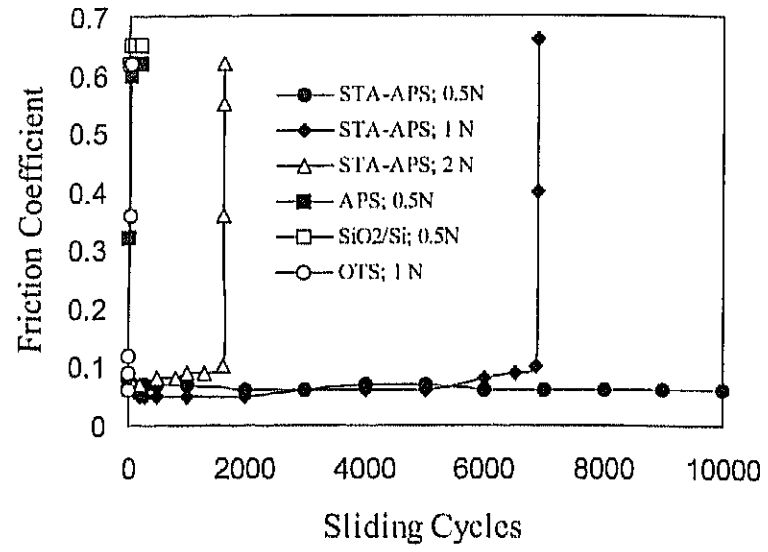

Figure 6. Variation in the friction coefficients with sliding cycles for various surfaces sliding against a Si_3N_4 ball at a sliding velocity of 90 mm/min (RH = 45%).

the friction-versus-load curve shows linear characteristic at high loads. The convex-shaped friction curve is found only in the low-load region, which might reflect that the value of 72 nN is not the true adhesion force (noting that the external load in Figure 5 is only up to about 45 nN). In other words, large difference between the pull off force and the adhesive force is observed (the pull off force is much larger than the true adhesive force in the present work). This might be attributed to that the capillary force would increase in the pulling off process of the tip from the surface. A simple example is that strong force is needed to pull off two pieces of glass combined with water entrapped in the interface. Nevertheless, the pull off force could still be used to compare the adhesive behavior of various surfaces, though it is not the true adhesion.

On the APS surface, the jump of the tip onto the surface becomes weak and the convex-shaped friction curve is only shown in the low-load range up to 5 nN. Contrary to the above, no jump is found on the STA–APS dual-layer film surface, and the whole curve is linear. This indicates that the STA–APS film had excellent micro-tribological properties and greatly reduced the adhesion and friction.

3.3 Macro-Tribological Behavior Characterization. The macro-tribological behaviors of the APS monolayer and STA–APS dual-layer film are shown in Figure 6. Surprisingly, unlike the corresponding AFM/FFM results shown in Figure 5, APS monolayer does not show any macrolubricity (A friction coefficient about 0.62 is registered after several sliding cycles, which is almost the same as that of the silicon surface). The static Hertzian contact stress for the Si_4N_3 ball of radius 2 mm at a normal load of 0.5 N is estimated to be about 0.7 GPa, which is roughly equal to the pressure under the AFM measurement (a rough estimation that a normal load of 40 nN corresponds to a pressure about 0.7 GPa for an AFM Si_4N_3 tip of radius about 50 nm according to ref 24). However, the macroscopic Si_4N_3 ball has a relatively rough surface and might experience multiasperity contact in the sliding process, namely, the pressure applied on the asperities, especially on the high ones, will be much larger than the Hertzian contact stress 0.7 GPa. In organic monolayer or multilayer films, an important stabilizing factor is the attractive forces from the van der Vaals interactions between the molecular chains, which play an essential role in ensuring condensed and robust packing.[24] Thus, it could be expected that the APS monolayer is poor ordering and mechanical stabilization would be weak and liable to fail under high pressure.

On the other hand, the STA–APS dual-layer film shows good frictional-reducing behavior and considerably high-

(24) Xiao, X. D.; Hu, J.; Charych, D. H.; Salmeron, M. *Langmuir* **1996**, *12*, 235.

load-carrying capacity. The friction coefficient is about 0.06 ~ 0.08 and the antiwear life is more than 10 000 cycles, about 6800 cycles, and about 1600 cycles, corresponding to the normal load of 0.5 N, 1 N, and 2 N, respectively. In a previous study of the SAMs of OTS, wear easily occurred after tens of sliding cycles under the normal load of 0.5 N; furthermore, it was liable to fail at a load of 1 N (Figure 6).[16] Noting that the OTS monolayer and the STA–APS dual-layer film have similar film thickness and bond mode with the substrate, it was supposed that the much different antiwear ability of them might be resulted from their different structures. In other words, the STA–APS film has a two-layer structure of which the defects can be compensated by the layered structure. At the same time, the mechanical stability of STA–APS film can be enhanced by the hydrogen bonds between the molecules, as shown in Figure 1, which is not available in the OTS monolayer. The mechanical advantages of multilayer inorganic coatings on engineering surfaces have been intensively focused on.[25,26] The similar studies, however, on the multilayer organic films are less available. Therefore, increased attention should be paid to the research in this respect, so as to reveal more insights into the correlation between the structure and properties of the ultrathin organic films.

The morphologies of the worn surfaces of the silicon wafer and STA–APS film after sliding against the Si_4N_3 ball observed with SEM are shown in Figure 7, that of the OTS monolayer worn surface is also shown in Figure 7 for a comparison. The bare silicon surface is characterized by severe plastic deformations and fractures after 100 sliding cycles under a normal load of 0.5 N (Figure 7a). The worn surface of the STA–APS film after 1000 sliding cycles under a normal load of 1 N shows signs of mild scratching (Figure 7b), while the worn surface of the OTS monolayer after 100 sliding cycles under 0.5 N (Figure 7c) shows signs of OTS accumulations. The above observations of the worn surface morphologies agree well with the corresponding wear resistance of the STA–APS dual-layer film and the OTS monolayer, that is, the STA–APS dual-layer film has much better friction-reducing and antiwear properties than the OTS monolayer.

The micro- and macro-tribological behavior of the films were examined at different relative humidities (the former was tested at a relative humidity of 65%, while the latter tested at 45%), but this does not lead to confusion to our present conclusions. Humidity does have a significant effect on the tribological properties, especially on the microscopic scale, but it is not feasible to compare the micro-tribological behavior of the film to the macro one. In other words, it is irrational to compare them directly even at the same humidity. This is why we discuss and interpret the micro and macro results, respectively, other than comparing them directly. Furthermore, no obvious effect of humidity on the macro-tribological properties of the dual-layer film has been found in our experiments.

4. Conclusion

In conclusion, a novel self-assembled dual-layer film was prepared by chemical adsorption of STA molecules onto the self-assembled monolayers of APS with terminal amino group on single-silicon crystal substrate. The STA–APS film has good adhesive resistance and can greatly reduce the friction force in micro and macro scopes. Moreover, it registers much better load-carrying capacity and antiwear ability than the self-assembled monolayers of OTS in sliding against the ceramic counterface. Thus, the dual-layer self-assembled STA–APS film might find promising application in the lubrication of MEMS.

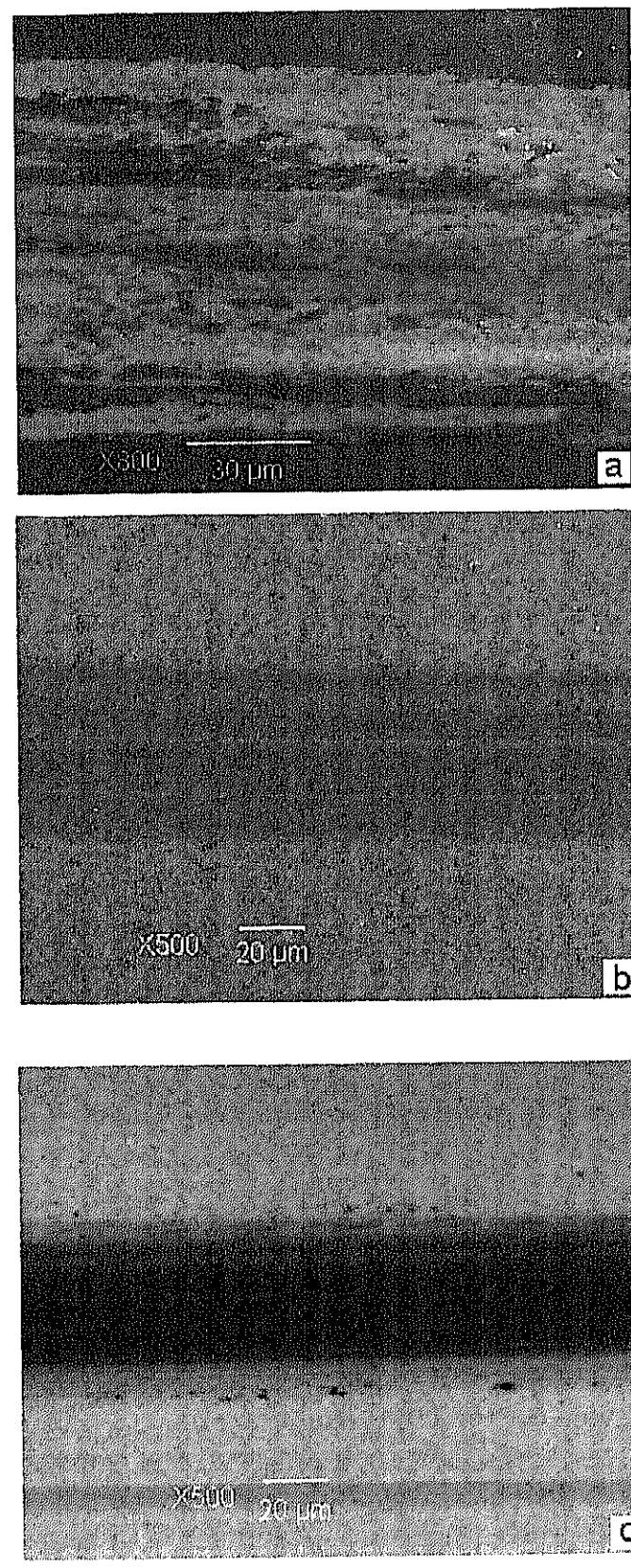

Figure 7. SEM images of the worn surfaces of the substrate and two film samples sliding against Si_4N_3 ball at different loads and sliding cycles, (a) bare silicon surface sliding for 100 cycles at 0.5 N, (b) STA–APS film sliding for 1000 cycles at 1 N, and (c) OTS monolayer sliding for 100 cycles at 0.5 N.

Acknowledgment. The authors would like to express their sincere thanks to Dr. Xudong Xiao (Department of physics, Hongkong university of technology and science) for his kindness of offering the AFM/FFM facility. We also wish to acknowledge the financial support from National Natural Science Foundation of China (Grant No. 50023001) and from the Chinese Academy of Sciences (Grant No. KJCX-SW-L2).

LA026662E

(25) Mal, K.; Bell, T.; Sun, Y. *Trans. ASME J. Tribology* **1997**, *119*, 476.

(26) Zhang, X.-S.; Yu, L.-G.; Chen, J.-M. *Tribology* **2000**, *20*, 156 (in Chinese).